

Signal enhancement in CRAZED experiments

Rosa T. Branca *, Gigi Galiana, Warren S. Warren

Department of Chemistry, Duke University, Durham, NC 27704, USA

Received 6 November 2006; revised 14 February 2007

Available online 31 March 2007

Abstract

Many of the promising applications of the CRAZED (COSY Revamped with Asymmetric Z-gradient Echo Detection) experiments are in biomedical and clinical technologies. In tissue, however, signal from the typical CRAZED experiment is largely limited by transverse relaxation. When relaxation is included, the maximum achievable signal from a prototypical CRAZED sequence, in the linear regime, is proportional to T_2/τ_d . This means that for samples with a short T_2 , as encountered in vivo, signals from intermolecular multiple-quantum coherences (iMQCs) reach very diminished signal intensities. While relaxation is generally regarded as a fundamental constraint, we show here that when T_2 is short but T_1 is long, as in tissue, there are simple sequence modifications that can increase signal beyond the T_2 limit. To better utilize the available signal intensity from iMQCs we propose a method to substitute part of the transverse magnetization with the longitudinally modulated magnetization. In this paper we show, with both simulations and experimental results, that in the presence of strong transverse relaxation the standard CRAZED scheme is not the optimal method for observing iMQCs, and can be improved upon with simple modifications.

© 2007 Elsevier Inc. All rights reserved.

Keywords: CRAZED; iZQC; iDQC; Dipolar demagnetization time

1. Introduction

Dipolar couplings between distant spins in solution can produce additional peaks in two-dimensional NMR experiments, corresponding to intermolecular multiple-quantum coherences [1–3]. In the last few years, these effects have evolved from a curiosity into a wide range of applications in imaging and high resolution spectroscopy. Recent applications include contrast enhancement in magnetic resonance imaging [4,5] and functional imaging [6,7], suppression of inhomogeneous broadening [8], measurements of local magnetization [9] or magnetization structure [10–12], and indirect detection [13], but are mainly limited by signal intensity. Analytic solutions for signal intensity from specific sequences have been available for some time, in the limit where relaxation can be ignored. Here we show, both numerically and experimentally, that the analytically

derived sequences are not optimal in the limit which is most appropriate for imaging ($T_2 \ll T_1$), and further signal enhancements are possible.

The prototype iMQC pulse sequence is the “CRAZED” sequence (Fig. 1), which can be shown analytically in either the classical or quantum pictures to give a signal of the form

$$M^+(\tau, t_2) = i^{n-1} e^{i\Delta\omega(t_2 - n\tau)} M_0 \sin \alpha_1 \times \left[\left(\frac{n\tau_d}{t_2 \delta_s \sin \alpha_1 \sin \alpha_2} \right) J_n \left(\frac{t_2 \delta_s \sin \alpha_1 \sin \alpha_2}{\tau_d} \right) - \frac{\cos \alpha_2}{2} J_{n+1} \left(-\frac{t_2 \delta_s \sin \alpha_1 \sin \alpha_2}{\tau_d} \right) + \frac{\cos \alpha_2}{2} J_{n-1} \left(-\frac{t_2 \delta_s \sin \alpha_1 \sin \alpha_2}{\tau_d} \right) \right]$$

where M_0 is the equilibrium magnetization, n is the coherence order being selected, $\Delta\omega$ is the resonance frequency offset, α_1 and α_2 are the flip angles of the excitation and mixing pulses, respectively, and J_m is the m th order Bessel

* Corresponding author.

E-mail address: rtb9@duke.edu (R.T. Branca).

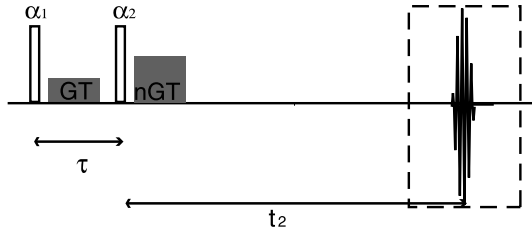


Fig. 1. Standard CRAZED pulse sequence used to observe iMQC. The first RF pulse α_1 , which excites the equilibrium magnetization, is followed by a delay τ and a gradient pulse of strength G and duration T which dephase the transverse magnetization. A second RF pulse α_2 transfers part of this oscillating magnetization along the z -axis creating the correct dipolar field to refocus the transverse magnetization. The ratio $(nGT)/(GT)$ also determines the selected coherence order.

function. The signal is scaled by a directional factor of $\delta_s = (3\cos^2\beta - 1)/2$, with β being the angle between the correlation gradient and the z -axis.

In this expression, $\tau_d = 1/(\gamma\mu_0M_0)$, called the dipolar demagnetizing time, sets the time scale for appearance of the iMQC resonances and is approximately 170 ms for tissue at room temperature in a 7 Tesla imager. If relaxation is not important, the theoretical upper limit of intermolecular zero quantum coherence (iZQC) signal, reached for an echo time of $2.6\tau_d$, is 41% of the magnetization [5]; intermolecular double-quantum coherence (iDQC) intensities can be even higher. However, both iZQC and iDQC signals grow linearly with the evolution time t_2 , and in most cases the theoretical maximum signals are heavily attenuated by relaxation and diffusion effects. When we include relaxation in the theoretical calculation of the iZQC signal, the time scale factor becomes the T_2/τ_d ratio, which for most biological samples is less than 1. This implies (Fig. 2) that the maximum signal achievable drops from the theoretical 40% to a few percent of the full equilibrium magnetization when we include relaxation. Nonetheless, this sequence has

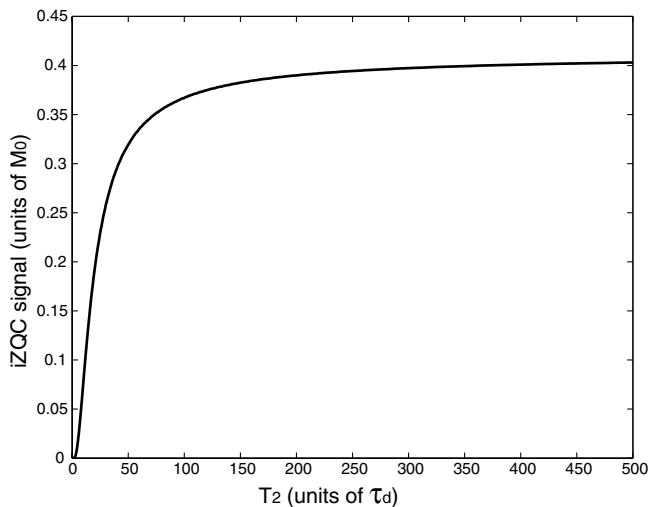


Fig. 2. iZQC maximum signal intensity in units of the equilibrium magnetization as a function of the normalized transverse relaxation T_2/τ_d .

still been used as the standard in virtually all iMQC experiments, and signal to noise ratio (SNR) is only improved by adding time consuming averages.

Here, we ask a different question: is CRAZED the right prototype sequence in the limit where relaxation dominates? In fact, straightforward arguments suggest that improvements are possible. For simplicity, we will consider here only the cases of zero- and double-quantum CRAZED sequences, and start with a qualitative explanation of why signal is produced. In the classical picture, the observed signal comes from interaction between longitudinal magnetization (whose modulation is determined only by the first gradient pulse) and transverse magnetization (whose modulation is determined by the first and second gradient pulses). If the modulation patterns are correctly aligned, the modulated longitudinal magnetization (which changes the local resonance frequency in a spatially well defined way) causes the modulated transverse magnetization to “bunch up” and produce a nonzero average. While this description is formally correct, it is easier to see what is happening in the quantum picture: operators of the form $I_{yi}I_{zj}$ are converted by distant dipolar couplings into operators of the form I_{xi} . If the modulation patterns of transverse and longitudinal magnetization are adjusted correctly, the $I_{yi}I_{zj}$ terms have a spatial modulation of the form $\cos(\gamma GT(z_i - z_j))$ which depends only on relative position. Since the dipolar couplings also depend on direction, the net effect can be nonzero magnetization.

In either picture, it is clear that the signal intensity will be decreased by either T_2 or T_1 relaxation. If $T_2 \ll T_1$ (as happens in virtually all MRI experiments), for times long compared to T_2 the transverse magnetization is dissipated, but modulated longitudinal magnetization remains. An additional pulse would turn some of the longitudinal into transverse, and again both magnetizations are well spatially correlated. Thus, in principle, more signal could be recovered by dipolar evolution, even though the system has not been restored to equilibrium.

2. Results and discussion

In order to test our approach we have simulated the signal behavior for the modified iZQC sequence for a homogeneous sample. The simulations were performed by numerically integrating the modified Bloch equations based on the finite element method and a Runge–Kutta algorithm [14,15]. The simulated sample was a $[32 \times 32 \times 32]$ array of voxels: $24 \times 24 \times 24$ grid points with magnetization density equal to 100% were surrounded by a 4 grid point shell of empty space (Fig. 3). To avoid edge effects the result of the simulations was then extracted only from the inner $[16,16,16]$ core. The size of the sample was $[1,1,1]$ cm. The correlation gradient was set along the z direction, and each helix was defined by 8 grid points. The resonant frequency of the spin was 165 MHz, the sample temperature 300 K, and the calculated dipolar demagnetizing time was 240 ms. The truncation error of the fifth-order

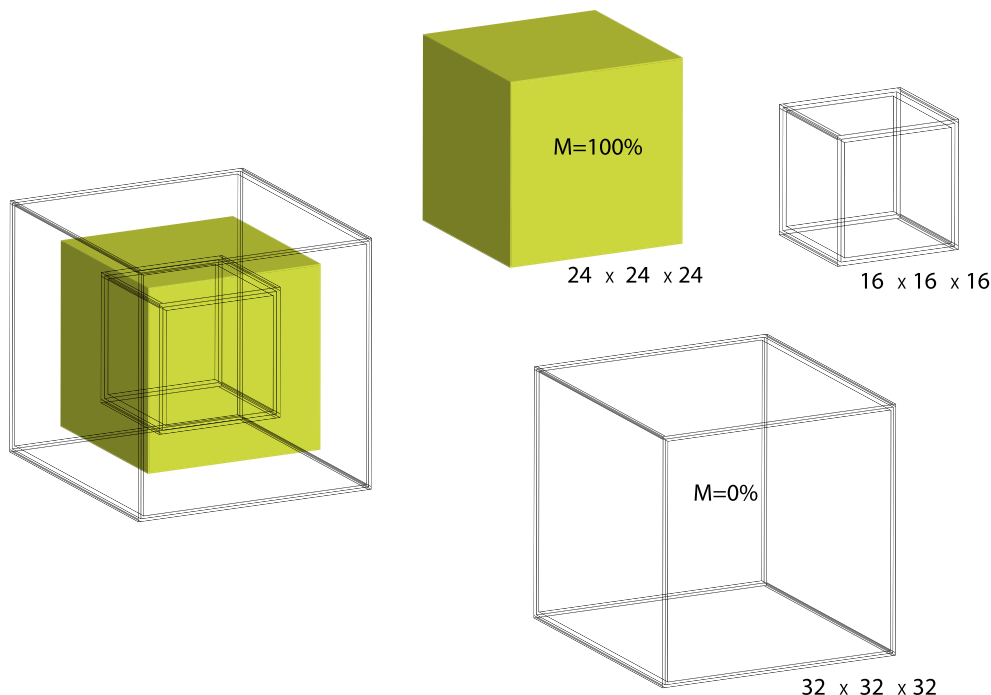


Fig. 3. Shape of the sample used in the simulations. The simulated region is a $32 \times 32 \times 32$ cube: an inner $24 \times 24 \times 24$ cube with magnetization density = 100% is surrounded by empty space. The result of the simulations is extracted only from a $16 \times 16 \times 16$ inner cube.

Cash–Karp Runge–Kutta integration method was kept below 10^{-10} in order to achieve a high calculation speed and adequate accuracy. In our simulations, we considered dipolar field evolution, and transverse and longitudinal relaxation, with a T_2 much lower than T_1 ($T_2 = 50$ ms and $T_1 = 1000$ ms). The sequence used for the simulations is displayed in Fig. 4. The pulse flip angle θ and the delay Δ between the last two pulses was varied in order to find the optimum values for the sample characteristics, while the τ delay was kept constant and equal to 2.1 ms. A two step phase cycle on the excitation pulse was used to select only the iZQC signal and cancel any SQC contamination. Specifically, the phase of the first excitation pulse ($\alpha_1 = 90^\circ$) was changed from $+x$ to $-x$, and the results of the simulations were coadded. In both steps, the phase of the mixing

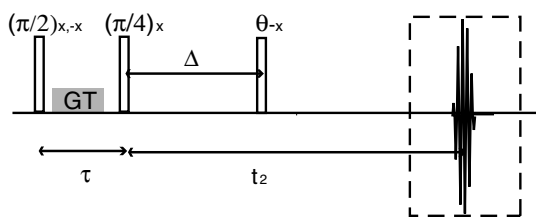


Fig. 4. Modified CRAZED pulse sequence to enhance the iZQC signal. The first 90° pulse excites multiple-quantum coherences. The second RF pulse, the mixing pulse, transfers part of the modulation onto the z -axis. During the acquisition time, the transverse magnetization evolves under the effect of the dipolar field created by the modulated I_z magnetization and a signal is observed. After the Δ delay, a third RF pulse, θ , with opposite phase of the mixing pulse, is used to substitute part of the lost transverse magnetization with the longitudinal magnetization.

pulse ($\alpha_2 = 45^\circ$) was set to $+x$ while the phase of the θ° pulse was set to $-x$. The simulation results for the sequence in Fig. 4 are shown in Fig. 5. A signal improvement up to 12.4% with respect to the standard CRAZED signal was observed for $\theta^\circ = 20^\circ$ and $\Delta = 40$ ms. Changing the mixing pulse from 45° to 120° and selecting a θ pulse in phase with the mixing pulse allowed us to obtain a signal enhancement up to 20% for $\theta^\circ = 25^\circ$ and $\Delta = 40$ ms (Fig. 6).

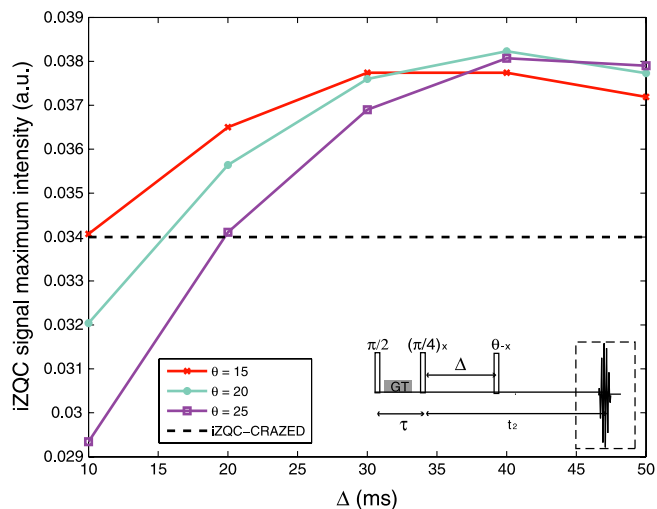


Fig. 5. Simulated iZQC signal intensity, from the sequence in Fig. 4, as function of the Δ delay for different θ° pulses. In this case the delay τ was set to 2 ms, and the mixing pulse was a $\pi/4$ RF with an opposite phase respect to the θ° pulse. The maximum signal enhancement is obtained for $\theta^\circ = 20^\circ$ and $\Delta = 40$ ms.

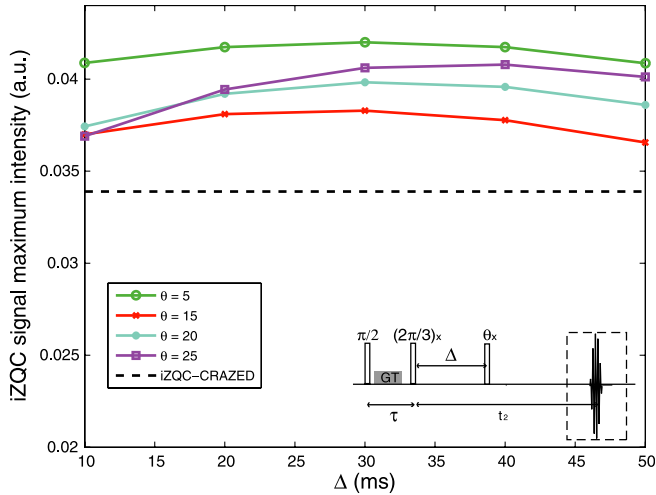


Fig. 6. Simulated iZQC signal intensity, from the sequence in Fig. 4. In this case the mixing pulse was changed to a 120° pulse in phase with the θ° pulse, and the maximum signal intensity was obtained for $\theta^\circ = 5^\circ$ and $\Delta = 30$ ms.

The same simulations were also run for a modified iDQC-CRAZED pulse sequence (Fig. 7), using the same sample characteristics of the previous simulations. A two steps phase cycle was again performed on the first pulse, changing it from $+x$ to $-x$ and adding the results. In this case, a signal enhancement was obtained when both the θ pulse and the 120° mixing pulse were in phase along $+x$.

As shown in Fig. 8, the simulations gave a maximum signal enhancement for $\theta^\circ = 15$ and $\Delta = 30$ ms. From these simulations, it is clear that the optimal flip angle for the θ pulse and the optimal delay, Δ , between the θ and mixing pulses depends not only on the characteristic relaxation times (T_1 and T_2) of the sample, but also on the order of the selected coherence (iDQC versus iZQC). Moreover, the relative phases of the mixing and θ pulses must be chosen carefully in order to get a signal enhancement. The evolution into observable signal proceeds differently for different coherence orders, therefore it is not surprising that these signals are optimized by different conditions.

Experimental data was also acquired using the modified version of the CRAZED pulse sequence (Fig. 4) on a 7 T horizontal-bore magnet equipped with a Bruker console. The sample consisted of two tubes, one filled with gel (left in Fig. 9) and the other filled with a mixture of gel and super paramagnetic iron oxide nanoparticles (right in

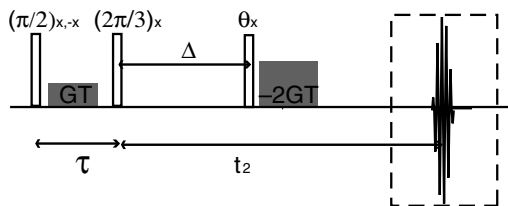


Fig. 7. Modified CRAZED pulse sequence to enhance the iDQC signal. In this case a signal enhancement is obtained when the third RF pulse, the θ° pulse, is in phase with the 120° mixing pulse.

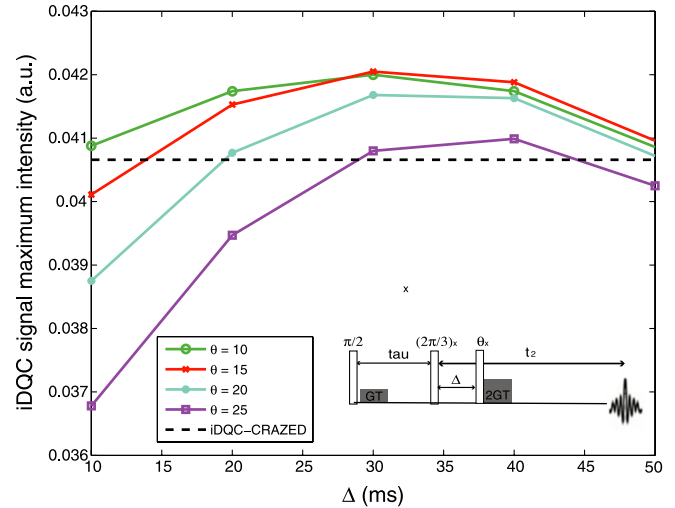


Fig. 8. Simulated iDQC signal intensity, from the sequence in Fig. 7, as a function of the Δ delay for different θ° pulses.

Fig. 9), both oriented along the static magnetic field direction. Measured T_1 and T_2 values were 1035 and 170 ms (respectively) for the gel sample, and 700 and 75 ms for the gel/nanoparticle mixture. A standard iZQC-CRAZED image of the sample was acquired (Fig. 9a). For the modified CRAZED experiments, both the θ pulse flip angle and the Δ delay were varied, while the time between the mixing pulse and the acquisition, t_2 , was kept constant, equal to 50 ms. The experimental results confirmed the same trend for the signal behavior as seen in the simulations: the signal was observed to increase, have a maximum, and then decrease as the flip angle θ and the delay Δ were increased further. However, for the two samples, the signal intensity was optimized for different values of θ and Δ . In particular, the signal for the plain gel showed a maximum intensity for $\theta^\circ = 15^\circ$ and $\Delta = 5$ ms (Fig. 9b), while the signal for the gel with nanoparticles presented a maximum intensity for $\theta^\circ = 15^\circ$ and $\Delta = 20$ ms (Fig. 9c). For comparison, all the iZQC images are displayed at the same image intensity scale.

Experimental results were also acquired using the modified version of the iDQC-CRAZED pulse sequence on the gel/nanoparticle phantom. In this case, the modified iDQC-CRAZED sequence was modified with respect to the simulation sequence by substituting the second gradient pulse (2G) with a couple of gradient pulses of opposite directions ($-4G$ and $+2G$). This modification compensates for chemical shift evolution and allows all iDQCs that follow two different pathways to refocus at the same position (Fig. 10b). For these experiments we chose $\tau = 4$ ms and $\Delta = 10$ ms. The experimental iDQC signal behavior for the modified CRAZED sequence (Fig. 10b), is shown in Fig. 11 as a function of the θ pulse alongside the experimental iDQC signal from the standard CRAZED sequence (Fig. 10a). In this case an enhancement of the signal up to 11% is observed for $\theta^\circ = 22^\circ$. Moreover going from higher to lower flip angle, a phase change of the signal is observed.

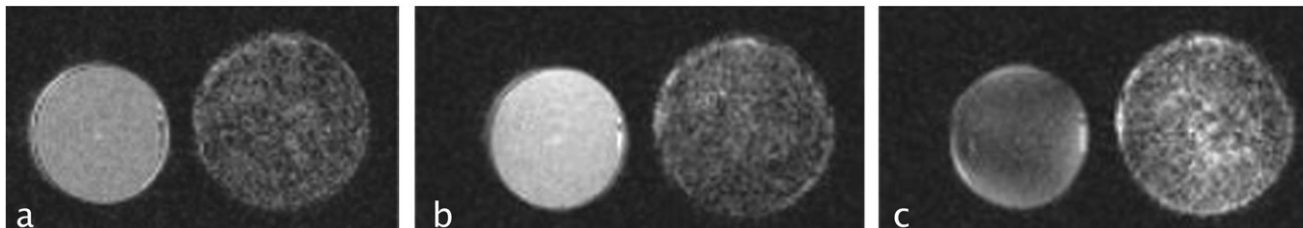


Fig. 9. iZQC-CRAZED images of a two tube sample: (a) standard iZQC CRAZED image; (b) modified iZQC-CRAZED image with $\theta^\circ = 15^\circ$ and $\Delta = 5$ ms; (c) modified iZQC-CRAZED image with $\theta^\circ = 15^\circ$ and $\Delta = 20$ ms.

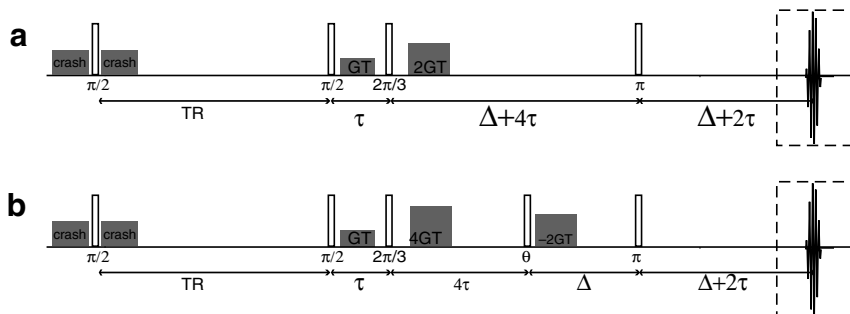


Fig. 10. (a) Standard CRAZED pulse sequence used to detect the reference iDQC signal in Fig. 11. (b) Modified CRAZED pulse sequence used for the experiments results of Fig. 11 to enhance iDQC signal. For the experiments in Fig. 11, the following parameters were used: $\tau = 4$ ms, $TR = 4$ s, $NA = 8$, and $GT = 8.4$ Gauss*ms/cm. For the modified sequence Δ was set to 10 ms, while the θ pulse was changed from 5° to 125° .

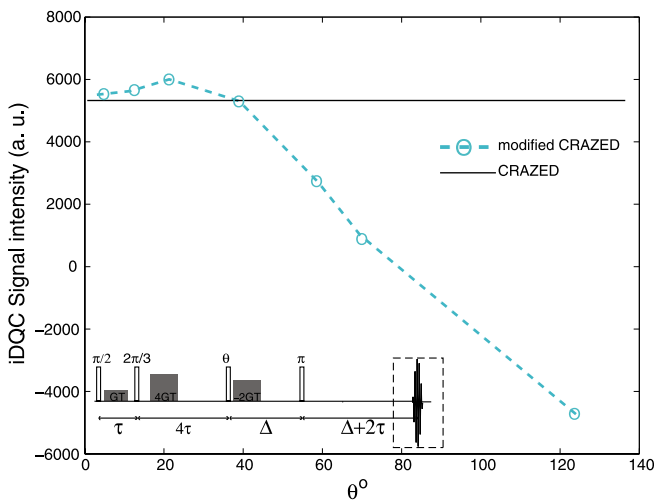


Fig. 11. Magnitude of the iDQC signal as function of the third RF pulse flip angle for the gel and nanoparticles samples. The straight line represents the reference maximum signal obtained with the standard iDQC-CRAZED pulse sequence (Fig 10a). The dotted line represents the experimental values of the iDQC signal obtained with the modified version of the CRAZED pulse sequence (Fig 10b) for different values of the θ pulse.

3. Conclusion

To date the successful application of biomedical iMQC MRI and spectroscopy has been limited because signals originating from iMQCs have a much lower signal to noise ratio (SNR) than those of conventional single quantum

coherences. Several methods have been proposed to enhance the iMQC signal by slowing down the effective dephasing rate, such as locking the signal during the evolution time and reducing the apparent T_2 [16]. What we have shown here, with both experimental observations and simulated results, is that in samples where relaxation is an issue, substituting part of the transverse magnetization with the longer lived longitudinal magnetization is a better approach to maximizing iMQC signal. Particularly in samples where $T_1 \gg T_2$, such as in tissue, we can lessen the effects of relaxation by partially substituting T_1 with T_2 . This can be done either using a single extra pulse in the sequence, as shown here, or with a series of pulses following the mixing pulse. While simulations with more than one pulse have not yet produced more signal enhancement, we are still investigating the pulse shape and flip angle which will produce the maximum signal.

Nevertheless, this demonstrates that the previously accepted limit of iMQC signal due to the transverse relaxation is not unassailable and we can get better signal to noise with very simple modifications. We do not suspect we have found a global optimum; we expect that, with further optimization, this and similar methods could lead to improved SNR in vivo without increasing the scan time.

Acknowledgment

This work was supported by the NIH under Grant EB 02122.

References

- [1] Q. He, W. Richter, S. Vathyam, W.S. Warren, *J. Chem. Phys.* 98 (1993) 6779–6800.
- [2] W.S. Warren, W. Richter, A.H. Andreotti, S. Farmer, *Science* 262 (1993) 2005.
- [3] S. Ahn, W.S. Warren, S. Lee, *J. Magn. Reson.* 128 (1997) 114–129;
S. Ahn, S. Lee, W.S. Warren, *Mol. Phys.* 95 (1998) 769–785.
- [4] W.S. Warren, S. Ahn, R.R. Rizi, J. Hopkins, J.S. Leigh, M. Mescher, W. Richter, M. Garwood, K. Ugurbil, *Science* 281 (1998) 247–250.
- [5] J. Zhong, Z. Chen, E. Kwok, *Magn. Reson. Med.* 43 (2000) 335–341.
- [6] W. Richter, M. Richter, W.S. Warren, H. Merkle, P. Andersen, G. Adriany, K. Ugurbil, *Magn. Reson. Imaging* 18 (2000) 489–494.
- [7] Jianhui Zhong, Edmund Kwok, Zhong Chen, fMRI of auditory stimulation with intermolecular double-quantum coherences (iDQCs) at 1.5 T, *Magn. Reson. Med.* 45 (2001) 356–364.
- [8] S. Vathyam, S. Lee, W.S. Warren, *Science* 272 (1996) 92–96;
Y.Y. Lin, S. Ahn, N. Murali, W. Brey, C.R. Bowers, W.S. Warren, *Phys. Rev. Lett.* 85 (2000) 3732–3735.
- [9] S. Gutteridge, C. Ramanathan, R. Bowtell, *Proc. Int. Soc. Magn. Reson. Med.* 8 (2000) 268.
- [10] R. Bowtell, P. Robyr, *Phys. Rev. Lett.* 76 (1996) 4971–4974.
- [11] S. Capuani, G. Hagberg, F. Fasano, I. Indovina, A. Castriota-Scanderbeg, B. Maraviglia, In vivo multiple spin echoes imaging of trabecular bone on a clinical 1.5 T MR scanner, *Magn. Reson. Imaging* 20 (2002) 623–629.
- [12] C. Ramanathan, R.W. Bowtell, NMR imaging and structure measurements using the long-range dipolar field in liquids, *Phys. Rev. E* 66 (2002) 041201.
- [13] R. Bowtell, *J. Magn. Reson.* 100 (1992) 1–17.
- [14] T. Enss, S. Ahn, W.S. Warren, *Chem. Phys. Lett.* 305 (1999) 101–108.
- [15] S. Garrett-Roe, W.S. Warren, *J. Magn. Reson.* 146 (2000) 1–13.
- [16] G. Galiana, R.T. Branca, W.S. Warren, In ENC Conference Abstracts, 2006.